Bioconjugate Chemistry

Article

pubs.acs.org/bc

Chemoenzymatic Conjugation of Toxic Payloads to the Globally Conserved N-Glycan of Native mAbs Provides Homogeneous and Highly Efficacious Antibody–Drug Conjugates

Remon van Geel, Marloes A. Wijdeven, Ryan Heesbeen, Jorge M. M. Verkade, Anna A. Wasiel, Sander S. van Berkel, and Floris L. van Delft*

SynAffix BV, Pivot Park, Molenstraat 110, 5342 CC, Oss, The Netherlands

Supporting Information

ABSTRACT: A robust, generally applicable, nongenetic technology is presented to convert monoclonal antibodies into stable and homogeneous ADCs. Starting from a native (nonengineered) mAb, a chemoenzymatic protocol allows for the highly controlled attachment of any given payload to the N-glycan residing at asparagine-297, based on a two-stage process: first, enzymatic remodeling (trimming and tagging with azide), followed by ligation of the payload based on copper-free click chemistry. The technology, termed GlycoConnect, is applicable to any IgG isotype irrespective of glycosylation profile. Application to trastuzumab and maytansine, both components of the marketed ADC Kadcyla, demonstrate a favorable in vitro and in vivo efficacy for GlycoConnect ADC. Moreover, the superiority of the native glycan as attachment site was demonstrated by in vivo comparison to a range of trastuzumab-based glycosylation mutants. A side-by-side comparison of the copper-free click probes bicyclononyne (BCN) and a dibenzoannulated cyclooctyne (DBCO) showed a surprising difference in conjugation efficiency in favor of BCN, which could be even further enhanced by introduction of electron-withdrawing fluoride substitutions onto the azide. The resulting mAb-conjugates were in all cases found to be highly stable, which in combination with the demonstrated efficacy warrants ADCs with a superior therapeutic index.

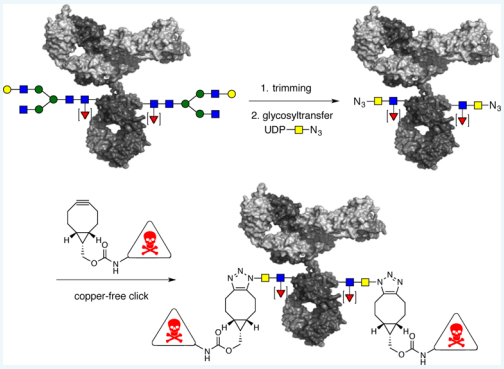

INTRODUCTION

More than 50 years after the first mice studies with an antibody–drug conjugate,[1] Ehrlich's dream[2] of the "magic bullet" for application in the field of oncology was recently realized with two ADCs receiving market approval: Adcetris (2011), a CD30-targeting ADC for treatment of Hodgkin lymphoma and sALCL, and Kadcyla (2013), a HER2-targeting ADC for breast cancer. The promising clinical results of both these marketed ADCs have tremendously boosted interest in targeted drug delivery for cancer treatment, with currently more than 40 ADCs in clinical development. The vast majority of ADCs in the clinic are based on conjugation of payload to naturally available amino acid side-chains (lysine, cysteine), leading to a stochastic distribution of drug–antibody ratio (DAR) between 0 and 8 (or even higher).[3] It has been demonstrated that random conjugation has a negative impact on efficacy,[4] and as a consequence the therapeutic index remains low (e.g., efficacious and maximum tolerated dose are similar for Kadcyla).[5,6]

Two main strategies can enhance the therapeutic index of a given mAb-payload combination: (a) site-specific conjugation[7] and (b) enhancing stability.[8,9] Site-specific conjugation is typically achieved by engineering of a specific amino acid (or sequence) into an antibody, serving as the anchor point for payload attachment.[10] However, re-engineering of protein sequence and site optimization is a laborious exercise. Moreover, expression yields may be compromised (typically ~50% yield reduction for a cysteine-engineered mAb,[11] while expression yields for genetic encoding of an unnatural amino acid typically reach 1 g/L maximally),[12,13] which has a significant impact on the cost of goods of the ADC. Finally, it has been amply demonstrated that ADCs obtained by conjugation to cysteine side chains often display limited stability in circulation, leading to premature disconnection of the cytotoxic payload before the tumor site is reached.[4] Some recent improvements in the field are notable,[8,9,14] however obviously still require a cysteine-engineered mAb.

Hence, ADC technologies should preferentially meet the following criteria: (a) use of native mAb (nongenetic approach), (b) control of conjugation site, and (c) delivery of a highly stable product. We report here a unique and robust chemoenzymatic technology for efficient mAb-to-ADC conversion by anchoring a payload to the antibody's glycan at

Special Issue: Antibody-Drug Conjugates

Received: April 21, 2015
Revised: May 25, 2015
Published: June 10, 2015

DOI: 10.1021/acs.bioconjchem.5b00224
Bioconjugate Chem. 2015, 26, 2233–2242

asparagine-297 (Figure 1A). By means of consecutive enzymatic glycan trimming and tagging of each N-glycan with

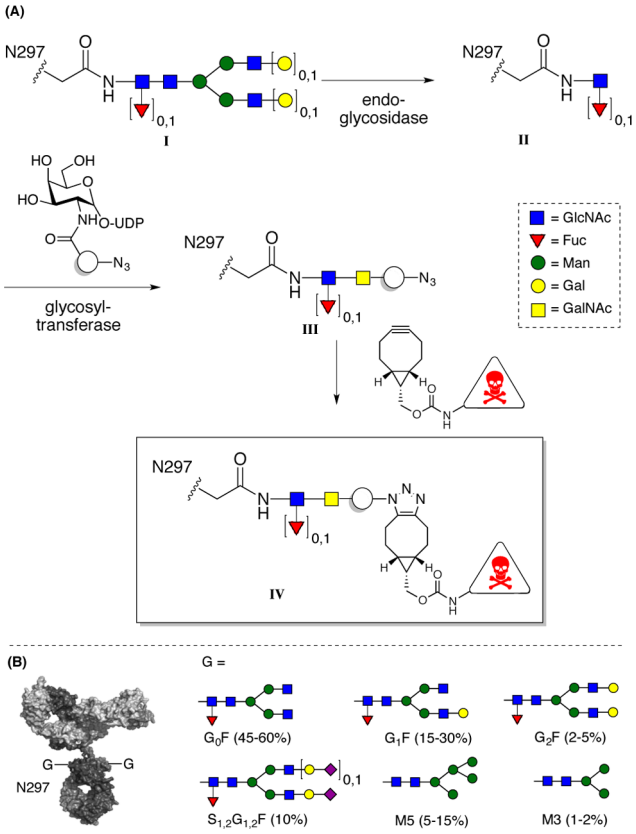

Figure 1. (A) Schematic depiction of ADC generation by chemoenzymatic remodeling: a native mAb (**I**, mixture of glycoforms at Asn-297) is trimmed by an endoglycosidase, thereby liberating the core GlcNAc (structure **II**). Next, an azido-modified GalNAc analogue is attached utilizing a glycosyl transferase (producing **III**). Third, the azido-modified glycan is subjected to copper-free click conjugation with a BCN-modified payload to provide ADC **IV**. (B) Main glycosylation forms of recombinant antibodies from CHO (with indication of abundance).[20]

precisely one azide, a unique anchor point is introduced for copper-free click conjugation with a payload. The versatility of this technology, termed GlycoConnect, is demonstrated across a range of different mAb isotypes and linker−payload combinations both in vitro and in vivo. Seamless upscaling of GlycoConnect corroborated manufacturability, whereas the superiority of the native glycosylation site for conjugation was demonstrated through in vivo efficacy assessment of a series of ADCs based on glycosylation mutants.

RESULTS AND DISCUSSION

All monoclonal antibodies are glycosylated at (or around) Asn-297. While variability of the glycan structure of an antibody exists within a single batch of mAb (Figure 1B), the exact ratio of isoforms differs per IgG isotype and is moreover highly dependent on the mammalian expression system used (CHO, sp2/0 or NS0).[15] Complex glycans (G0−2) typically dominate, largely fucosylated at the core GlcNAc, while >10% of galactose residues may additionally be sialylated and various levels of mannosylated glycans (5−17%) may be present.[16] The exact nature of the glycan is fundamentally important during antibody monotherapy by binding to Fcγ-receptors,[17] thereby inducing antibody-directed cellular cytotoxicity (ADCC) and/or complement-dependent cytotoxicity (CDC). For targeting therapy as with ADCs, however, effector function plays only a marginal role, whereas the presence of glycans may actually be considered disadvantageous due to reduced tumor-specific targeting as a result of uptake by FcγR-positive cells.[18] Off-target cellular uptake of the ADC by mannose receptors may be additionally disadvantageous.[19]

We reasoned that the globally conserved glycan may be rendered advantageous by serving as a natural anchor point for payloads. However, the heterogeneous nature of the glycan precludes the direct introduction of a defined number of payloads onto the glycan. For example, the first reported approach along this line involved periodate oxidation of terminal galactose residues, followed by oxime ligation of payload, which led to a wide distribution of different conjugates.[21] Qasba et al. were the first to demonstrate that, after prior convergence of different glycoforms to G0(F) upon galactosidase and sialidase treatment, chemoenzymatic fluorescent labeling of antibody could be effected with galactosyltransferase GalT(Y289L) and ketosugar **1** (Figure 2).[22,23]

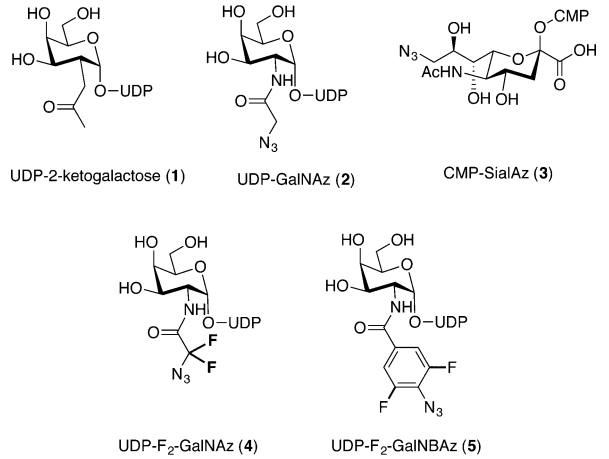

Figure 2. Previously reported (**1**−**3**) and new (**4**−**5**) UDP sugar substrates for chemoenzymatic remodeling of mAbs.

Lewis et al. also applied a chemoenzymatic strategy to J591, a PSMA-targeting antibody, with azido-modified GalNAc (GalNAz, **2**), followed by radiolabeling with strain-promoted azide−alkyne cycloaddition (SPAAC).[24] Finally, Boons et al. followed a two-stage approach for ADC generation of a CD22-targeting antibody via conversion of G0(F) to G2(F) isoforms by enzymatic galactosylation, followed by enzymatic introduction of C9-azido-modified sialic acid (SialAz, **3**) and subsequent copper-free click conjugation of payload with a dibenzoannulated cyclooctyne (DIBO).[25] The above chemoenzymatic strategies, by virtue of the branched nature of G0, all generate ADCs with DAR4, which may not always be desirable, for example, when extremely potent and/or lipophilic payloads are employed, e.g., pyrrolobenzodiazepine (PBD) dimers. Moreover, the high lipophilicity of the resulting ADCs, further enhanced in case a benzoannulated cyclooctyne is applied, may lead to increased aggregation and accelerated hepatic clearance from circulation. Finally, it must be noted that mannosylated glycoforms (typically 5−17%) are not converted into an ADC based on the above protocols.

DOI: 10.1021/acs.bioconjchem.5b00224
Bioconjugate Chem. 2015, 26, 2233−2242

We set out to investigate a chemoenzymatic ligation strategy to generate DAR2 ADCs, based on the strategy depicted in Figure 1: (1) trimming of *all* glycan isoforms (complex, hybrid, high-mannose) with an endoglycosidase, thereby liberating the core GlcNAc; (2) enzymatic transfer of a galactose residue harboring a reactivity-enhanced azide to reduce conjugation stoichiometry and incubation time; and (3) copper-free click conjugation with bicyclononyne (BCN), a cyclooctyne with minimal lipophilicity to reduce aggregation.

Endoglycosidase Treatment. As described above, a mAb obtained by recombinant expression in a mammalian system will display high glycan heterogeneity. While the main glycan isoforms of a mAb expressed in CHO are depicted in Figure 1B, recombinant expression in other mammalian cells (Sp2/0, NS0) typically further enhances heterogeneity due to formation of varying amounts of hybrid, bisected, α-galactosylated, and N-sialylated glycans.[16] Thus, effective trimming of all N-glycans present on any IgG requires access to an endoglycosidase with excellent substrate tolerability. In addition, high activity of the endoglycosidase (or more precise: endo-β-*N*-acetylglucosaminidase) is of course also desirable. With this in mind we selected glycosidases with high glycan tolerability and reported IgG activity, i.e., endo F3, endo S, and endo S2. As model antibodies, we used trastuzumab, with a single glycosylation site at Asn-300, and cetuximab, which belongs to the ~20% of mAbs harboring two glycosylation sites (one at Asn-299 and one at Asn-88).[26]

Endo F3 is known to cleave a wide variety of complex glycans, but not oligomannose and hybrid structures and has 400-fold lower activity on nonfucosylated glycans.[27] Indeed, we found that upon incubation of trastuzumab with endo F3, the majority of glycans was readily removed, but full trimming was not attained, even with large excess of enzyme. A similar situation occurred with endo S,[28,29] which is highly active—even with nonfucosylated glycans—but fails to hydrolyze oligomannose structures. Finally, we anticipated that endo S2 would display the desirable combination of substrate tolerability and activity.[30] Indeed, incubation of trastuzumab with only 1% (w/w) of enzyme was sufficient for full hydrolysis of the glycans, including oligomannose structures, as judged by SDS-PAGE and mass spectrometric analysis (Supporting Information).

Galactosyl Transferase. In 2002, Qasba et al. reported that a single mutation of a wild-type galactosyltransferase, GalT-(Y289L), resulted in excellent transferase activity of *N*-acetyl-D-galactosamine (GalNAc)[31] and could also be applied to transfer a 2-keto-derivative of galactose (**1**, Figure 2) onto a GlcNAc substrate.[32] For the highly similar polypeptide-galactosaminyl-transferase, Bertozzi et al. showed that the azido-modified GalNAc analogue GalNAz (**2**, Figure 2) is an effective substrate.[33] These observations were elegantly combined by Lewis et al. in 2013, showing that GalT(Y289L) is also able to recognize and incorporate GalNAz onto glycoproteins.[24] We speculated that GalT(Y289L) may not only be effective in functionalization of the natural substrate for galactosylation—the terminal GlcNAc of complex glycans—but also be applied in transfer of GalNAz onto the mAb core N-GlcNAc liberated upon endoglycosidase treatment (structure **II** in Figure 1). Indeed, we found that incubation of trimmed trastuzumab (**II**) with GalNAz **2** (0.4 mM) in the presence of only 1% (w/w) of GalT(Y289L) and $MnCl_2$ (10 mM) led to complete labeling after overnight incubation, thereby effectively installing precisely two azide groups (one per heavy chain) onto the antibody (i.e., structure **III** in Figure 1 labeled with galactose derivative **2** as depicted in Figure 2, denoted as **III-2**).

Click Conjugation/Choice of Cyclooctyne. Having successfully obtained bis-GalNAz-modified trastuzumab (**III-2**), the stage was set to investigate the conjugation of a functional group by means of click chemistry. Our initial investigations focused on the use of copper-mediated click chemistry. To this end, trastuzumab $(GalNAz)_2$ **III-2** was incubated with commercially available propargyl (+)-biotin derivative **6** (Figure 3), in the presence of $CuSO_4$ and Na-

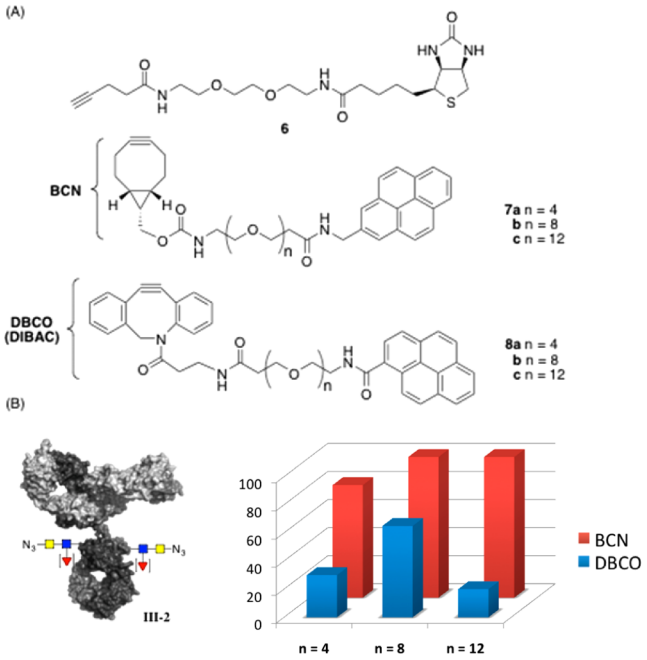

Figure 3. (A) Structures of propargyl-(+)-biotin (**6**), BCN-PEG$_n$-pyrene (**7a–c**), and DBCO-PEG$_n$-pyrene (**8a–c**) constructs. (B) Conjugation efficiency of cyclooctynes, depending on PEG chain length, for **7** and **8**.

ascorbate (Supporting Information). While complete labeling was observed after overnight incubation, as corroborated by MS analysis, a close inspection of the mass profile of the adduct, in particular after enzymatic digestion, indicated that several amino acids (His-288, Met-4) had suffered from partial concomitant oxidation. Although careful optimization of reaction conditions could possibly annihilate undesired amino acid oxidation, it was reasoned that such optimization would need to take place on case-by-case (mAb) basis, since even small amounts of oxidized protein may induce immunogenic response. An elegant solution to avoid copper involves train-promoted chemistry with cyclooctynes, as originally applied by Bertozzi et al.[34] However, the low reaction rate constants of the original cyclooctynes urged the development of a whole range of improved cyclooctynes over the years.[35] Some of us (S.V.B., F.V.D.) contributed to the field (2010) bicyclo[6.1.0]nonyne (BCN)[36] and dibenzoazacyclooctyne (DBCO, originally named DiBAC),[37] two cyclooctynes with a significantly improved reactivity profile, which have nowadays firmly established themselves in the field of strain-promoted azide–alkyne cycloaddition.

We anticipated that copper-free conjugation would fully avoid the aforementioned undesired amino acid oxidation. Thus, we prepared a range of derivatives (Figure 3A) of BCN-

DOI: 10.1021/acs.bioconjchem.5b00224
Bioconjugate Chem. 2015, 26, 2233–2242

Table 1. Overview of Conditions and Conjugation Efficiencies of Azido-Modified Trastuzumab Variants III-2, III-4, and III-5 with a Range of BCN-Linker Payload Constructs[a]

entry	UDP-sugar	linker	payload	equiv	cosolvent	amount (%)	conversion (%)
1	GalNAz (**2**)	PEG_8	doxorubicin	2	DMF	5	>95
2		PEG_2-glut-vc-PABA	MMAE	5		5	>95
3		PEG_2-glut-vc-PABA	MMAF	1.5		5	>95
4		PEG_4-Ahx	maytansine	2		5	90
5		PEG_2-vc-PABA-β-Ala	maytansine	2.5		25	60
6		PEG_4-vc-PABA-DMEDA	duocarmycin SA	1.5		12.5	85
7	F_2−GalNAz (**4**)	PEG_2-glut-vc-PABA	MMAF	4	DMSO	5	>95
8		PEG_4-Ahx	maytansine	3	DMA	5	>95
9		PEG_2-vc-PABA-β-Ala	maytansine	3	DMF	5	>95
10		PEG_4-vc-PABA-DMEDA	duocarmycin SA	3	DMA	2.5	>95
11	F_2−GalNBAz (**5**)	PEG_4-Ahx	maytansine	3	DMA	5	>95
12		PEG_2-vc-PABA-Ahx	maytansine	3		5	>95
13		PEG_2-glut-vc-PABA	MMAF	4	DMSO	5	>95

[a]Full structures of the Linker-Payloads can be found in the Supporting Information. PEG = polyethylene glycol, glut = glutaryl, vc = Val-Cit, PABA = *p*-aminobenzylalcohol, Ahx = 6-aminohexanoyl, DMEDA = *N,N′*-dimethylethylene diamine, MMAE = monomethyl auristatin E, MMAF = monomethyl auristatin F.

pyrene (**7**) and DBCO-pyrene (**8**), separated by a range of ethylene glycol linkers of different length (n = 4, 8, 12). Pyrene was selected to mimic the typically hydrophobic payloads needed for ADC purpose, while the PEG-linkers of different chain length were included to evaluate their potential to facilitate conjugation of the hydrophobic pyrene and cyclooctyne moieties. In addition, we compared conjugation efficiency of both BCN and DBCO under aqueous conditions, in particular, in light of the anticipated higher reactivity of DBCO versus BCN (for aliphatic azides), but also due to the much greater hydrophobic nature of the former. Hence, trastuzumab$(GalNAz)_2$ **III-2** (Figure 3) was incubated with **7a−c** or **8a−c** and progress of the reactions was monitored by mass spectrometry (Supporting Information). As anticipated, conjugation of BCN-PEG-pyrene gradually improved by increasing PEG chain length from 4 to 8 ethylene glycol units (no further improvement was observed for PEG_{12}). A similar trend was noted for conjugation of DBCO-PEG_n-pyrene (n = 4 or 8); however, much to our surprise further increase in ethylene glycol chain length to 12 in fact thwarted the conjugation process, which did not exceed beyond 20%.[38] The inability of DBCO to reach full conversion during SPAAC has in fact already been reported for labeling of monoclonal antibodies containing an azidoamino acid.[13] Nonetheless, in all cases it was found that SPAAC with BCN (reaching full conversion) was clearly favorable over DBCO (leveling off at max ∼60%). In addition, we established that ADCs containing DBCO show enhanced propensity to aggregate compared to their BCN-analogues (Supporting Information).

ADC Production and Stability. With all components in place (enzymes, substrate, and BCN), the stage was set to generate ADCs via our glycan remodeling−copper-free click strategy. Hence, we synthesized a range of BCN-linker-payload constructs, summarized in Table 1 (structures summarized in Supporting Information), with variation of linker (short/long, cleavable/noncleavable) and payload (monomethyl auristatins E and F, duocarmycin SA, maytansine).[39] As becomes apparent from Table 1 (entries 1−6) varying amounts of organic cosolvent were required, depending on linker-payload, to ensure full solubility during conjugation. In the majority of cases, 5% of DMF sufficed to ensure full conjugation (>95%) of BCN-linker-payload, although 12.5% was required for the highly hydrophobic BCN-PEG_4-vc-PABA-DMEDA-duocarmycin SA construct (entry 6). Shortening of the PEG linker, as in the BCN-PEG_2-glutaryl derivative (entry 5), not only required 25% of cosolvent, but also resulted in reduced conjugation efficiency (60%). It must be noted that, although all conjugations in Table 1 were performed on trastuzumab as model system, application to other mAbs afforded similar results (vide infra). Stability studies were performed by incubating ADCs based on MMAF and maytansine for a prolonged time in blood plasma (2 weeks, 37 °C), which showed no sign of degradation of linker in either case.[40] In addition, aggregation studies under similar conditions showed <1% formation of aggregates after 2 weeks in plasma at 37 °C for both ADCs (see Supporting Information). Our next objective was to demonstrate the scalability of the GlycoConnect technology. To this end, 5 g of Rituxan (rituximab), an antibody known to be less stable than trastuzumab, was subjected to the chemoenzymatic modification protocol. Much to our satisfaction, we found that upscaling GlycoConnect to increasing amounts of rituximab (5 mg → 100 mg → 1 g → 5 g) and subsequent conjugation with BCN-PEG_8-doxorubicin proceeded seamlessly, affording the desired ADC with excellent homogeneity (Supporting Information).

In Vitro and In Vivo Evaluation. Some of the ADCs prepared above were evaluated for their cell-killing potential on a Her2-overexpressing cell line (SK-Br-3) and compared to a Her2-negative cell line (MDA-MB231). As becomes clear from Figure 4, both maytansine- and MMAF-based ADCs showed

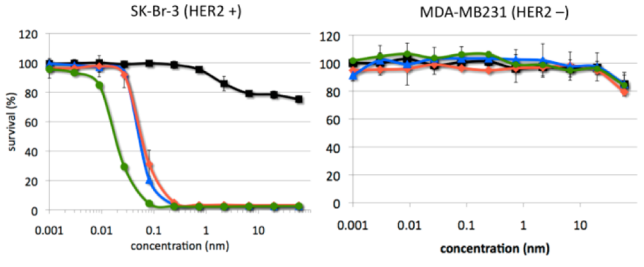

Figure 4. In vitro cytotoxicity of GlycoConnect ADCs based on vc-PABA-maytansine (blue line) and vc-PABA-MMAF (green line) versus Kadcyla (red line) and trastuzumab (black line).

DOI: 10.1021/acs.bioconjchem.5b00224
Bioconjugate Chem. 2015, 26, 2233−2242

comparable or better cytotoxicity than the benchmark Kadcyla, the marketed ADC that is also based on trastuzumab and maytansine hence only differs in conjugation technology.

The advantage of glycan-remodeled ADCs versus randomly labeled ADCs becomes even more apparent in vivo. To this end, PDX mice with an average tumor size of 100 mm^3 were intravenously injected with one of three different GlycoConnect ADCs (cleavable/noncleavable with maytansine or cleavable with MMAF) and compared to Kadcyla at 9 mg/kg (single dose bolus injection), followed by twice weekly tumor sizes measurements (Figure 5). During the first week, all groups

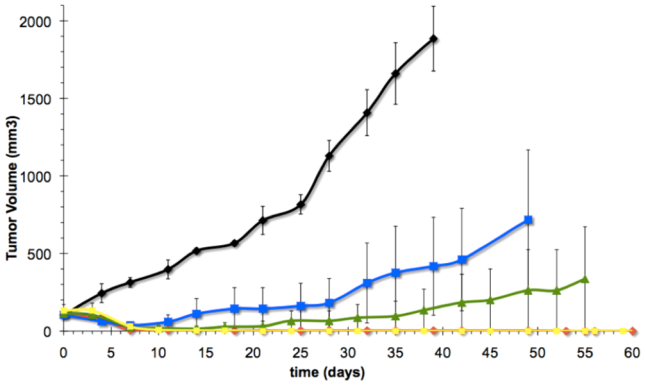

Figure 5. In vivo efficacy of GlycoConnect in a mouse HBCx-15 PDX xenograft with single injection (9 mg/kg) of trastuzumab-based ADCs. Full and permanent regression becomes apparent with maytansine-based ADCs, both with cleavable (Val-Cit-*p*-aminobenzylalcohol [vc-PABA], red line) or noncleavable linker (6-aminohexyl [Ahx], yellow line). Some tumor regrowth becomes apparent with vc-PABA-MMAF (green line), which is more prominent with Kadcyla (blue line). Black line is vehicle.

showed significant tumor shrinkage or even complete regression. After 1 week, tumor sizes gradually increased for mice treated with Kadcyla but not for any of the GlycoConnect ADCs. Only after approximately 3 weeks, reappearance and regrowth of tumors became apparent for mice treated with trastuzumab-vc-PABA-MMAF, while both ADCs based on maytansine (cleavable or noncleavable) showed complete tumor regression for the whole length of the study (60 days). This study thus clearly demonstrates the superiority of GlycoConnect conjugation technology versus a randomly conjugated ADC based on the same components. The latter observation becomes particularly interesting in view of the higher drug loading of Kadcyla (average DAR3.5)[3] versus GlycoConnect ADCs (DAR2).

Finally, it was established that glycan remodeling does not negatively impact pharmacokinetics. Although theory dictates that the mAb glycan plays no role in reshuttling of mAb by the FcRn receptor,[41] we felt it important to corroborate the latter also in the context of glycan-remodeled ADCs. To this end, trastuzumab (native and trimmed) and both trastuzumab-vc-PABA-based ADCs were (randomly) radiolabeled with ^{111}In and injected into mice. Samples were taken at preset time intervals and measured for residual radioactivity. As expected, no difference in blood clearance was observed (Supporting Information).

More Reactive Azido-Substrates. Recently, it was reported by van Delft et al. that reaction rate constants for SPAAC with BCN can be tremendously accelerated by applying electron-poor aromatic azides instead of the traditional aliphatic azides.[42] For example, it was demonstrated that an azidopyridinium derivative reacts >30 times faster than benzyl azide with BCN (but not with DBCO) following an inverse electron-demand mechanism. We speculated that a similar effect may be operative upon introduction of electron-withdrawing fluoride substituents on aliphatic azides, to potentially further enhance payload conjugation efficiency. Indeed, a competition experiment between model substrates $N_3CH_2C(O)NHBn$ and $N_3CF_2C(O)NHBn$ for reaction with BCN indicated a 2.3-fold higher activity of the difluorinated analogue (see Supporting Information). Based on this result, we designed and synthesized the difluorinated UDP-GalNAc derivative UDP-F_2−GalNAz (**4**, Figure 2) for evaluation in GlycoConnect. Enzymatic incorporation with GalT(Y289L) onto trimmed trastuzumab **II** (Figure 1) proceeded smoothly under standard conditions, to produce trastuzumab (F_2−GalNAz)$_2$ derivative **III-4**. Another competition experiment was performed, in this case involving incubation of equimolar amounts of nonfluorinated (GalNAz-based) **III-2** and difluorinated **III-4** with a substoichiometric amount of BCN-PEG_{2000} in PBS buffer, again indicating a >2-fold increase in reactivity for the difluorinated analogue (see Supporting Information). Encouraged by these results, we investigated whether GalT(Y289L) would also be able to incorporate the azide derivative of difluorinated *N*-benzoyl-D-galactosamine (F_2−GalNBAz, **5**, Figure 2), which based on our earlier study was expected to display a reaction rate constant at least 15 times higher than GalNAz. Initial remodeling experiments, under standard conditions, indicated only poor enzymatic incorporation of F_2−GalNBAz. However, increasing the concentration of UDP-substrate **5** to 5 mM and GalT(Y289L) to 15% (w/w) ensured full conversion of **II**, leading to quantitative formation of trastuzumab(F_2−GalNBAz) **III-5** as judged by mass spectrometry. In order to improve the activity of the galactosyltransferase, we designed and produced a small set of Y289 mutants. Interestingly, we found that one of these mutants, GalT(Y289M), dramatically enhanced the efficiency of incorporation of F_2−GalNBAz, which ensured full conversion into **III-5** under much improved conditions (150 μM GalT(Y289M) and 5 mM **5**).

With two difluorinated azido-trastumumab derivatives in hand, the stage was set to evaluate their suitability of ADC preparation. Thus, **III-4** (F_2−GalNAz) or **III-5** (F_2−GalNBAz) were incubated with BCN-Ahx-maytansine or BCN-vc-PABA-maytansine), with minimal reagent stoichiometry and low reaction times. In line with the enhanced activities of the respective azides, it was found that full conversion of **III-4/5** into **IV-4/5** could be ensured within 4 h using as little as 1.5 equiv of BCN-linker-toxin per azide. The enhanced reactivities of the difluorinated substrates may translate into significantly improved manufacturability (reduced stoichiometry and time in plant) and, hence, cost of goods.

Having generated most of our data with trastuzumab, a particular robust monoclonal antibody, we next moved to different monoclonal antibodies to demonstrate the applicability of GlycoConnect. First of all, we investigated the applicability of GlycoConnect on IgG2 and IgG4 isotypes. Both antibody formats are known to be susceptible to domain scrambling under reducing conditions, which are inevitable for any cysteine-based conjugation technology. Second, we evaluated GlycoConnect in the context of mAbs produced in Sp2/0 and NS0. A range of commercially available therapeutic antibodies was obtained: infliximab (IgG1 from Sp2/0),

DOI: 10.1021/acs.bioconjchem.5b00224
Bioconjugate Chem. 2015, 26, 2233−2242

palivizumab (IgG1 from NS0), panitumumab (IgG2 from CHO), and natalizumab (IgG4 from NS0). After dialysis to remove excipients, each mAb was subjected to our standard protocol for conversion into ADC and the process was followed by mass spectrometry. In all cases, clean and quantitative conversion into ADC was observed (Figure 6).

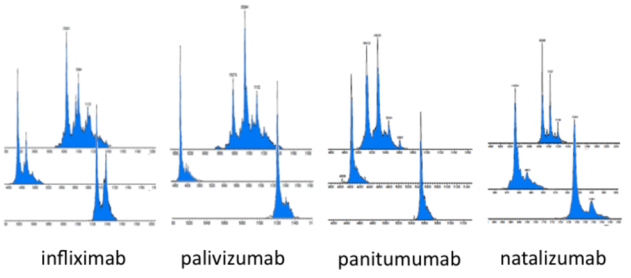

Figure 6. Mass spectral data (crude) of glycan-remodeling–conjugation of different IgG isotypes. Top row displays mass spectral profile of the heavy chain of native mAb, middle line after glycan remodeling (with F_2–GalNAz **4**), bottom spectrum after conjugation with a BCN-maytansine construct.

Site-Scanning Study. Finally, we set out to investigate if the native glycosylation site is indeed optimal in the context of efficacy. It has been amply demonstrated by others that there is a relevant correlation between conjugation site and ADC efficacy.[43] Most recently, it was demonstrated[44] that ADCs with cleavable linkers are significantly less *stable* in mouse plasma if not conjugated at or around Asn-297. The latter observation is highly inconvenient if a mouse xenograft model is used to assess ADC efficacy, although (presumably) not prohibitive for eventual clinical application in humans. Endorsing the importance of the site of conjugation, we performed a small site-scanning study for trastuzumab-based ADCs by engineering a new glycosylation site into trastuzumab heavy chain or light chain (based on the sequence N-X-S/T) and simultaneously mutating Asn-300 to Gln (trastuzumab numbering). The newly designed trastuzumab double mutants were transiently expressed in CHO and glycosylation was confirmed by mass spectrometry. Next, each individual trastuzumab mutant was subjected to endoglycosidase endo F3,[45] followed by enzymatic incorporation of F_2–GalNAz **4**, purification by protein A affinity chromatography, and SPAAC with BCN-PEG_4-Ahx-maytansine. The resulting, noncleavable ADCs were purified by size-exclusion chromatography and the resulting ADCs were injected into PDX mice at suboptimal dose (6 mg/kg) in order to be able to quantify differences in efficacy. We were pleased to find that, in accordance with previous reports, the most efficacious ADC (red line) was indeed derived from native trastuzumab Asn-300 (Figure 7). However, an important difference is that the set of ADCs investigated in our study involved solely noncleavable linkers, which excludes the role of a potential endogenous serine hydrolase in differentiating between the range of conjugates.[44]

CONCLUSION

A straightforward and robust technology for conversion of mAbs into ADCs has been developed, based on enzymatic remodeling of naturally present glycans, followed by copper-free click conjugation with BCN-payload constructs. The methodology is generally applicable to any recombinant IgG isotype, irrespective of mammalian expression system and

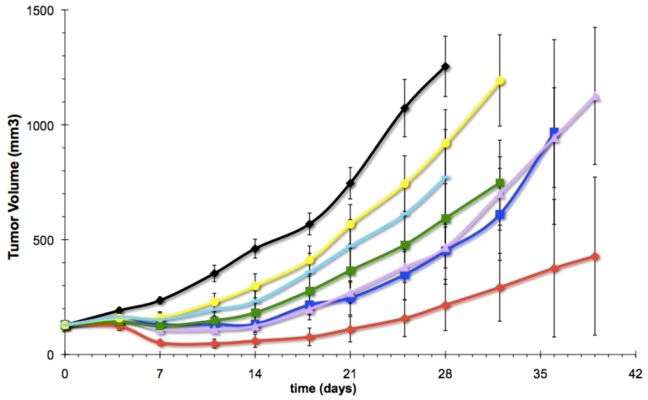

Figure 7. In vivo site-scanning of five different glycomutants demonstrating superior efficacy for the native glycosylation site (red line) compared to all glycosylation mutants included.

linker–payload combination. The resulting ADCs were found to be homogeneous and highly hydrolytically stable, while displaying negligible aggregation. Benchmark in vitro and in vivo efficacy studies against the marketed product Kadcyla, based on the same antibody and payload components, generated strong biological data in favor of the GlycoConnect ADCs, despite the lower DAR. The superiority of the natural mAb glycosylation site around Asn-297 was demonstrated in vivo by a side-by-side comparison of a range of trastuzumab glycomutants. Current efforts in our laboratory are focusing on the development of linkers with increased potential to accommodate highly lipophilic payloads (duocarmycins, PBD dimers) versus the commonly employed ethylene glycol linkers, which show only limited usefulness in this regard. Moreover, we are looking into branched linker formats that may allow for ADCs with higher DAR (4–8), and possibly even combinations of payloads with different modes of action, to combat multidrug-resistant tumors with a combination therapy-like approach. In summary, GlycoConnect technology is readily applicable to any off-the-shelf monoclonal antibody (turnaround in <1 week), while delivering site-specific, stable, and highly efficacious ADCs. We are confident therefore that GlycoConnect shows high promise as the next-generation ADC generation technology for targeted therapy with improved therapeutic index.

EXPERIMENTAL PROCEDURES

Solvents were purchased from Sigma-Aldrich or Fisher Scientific and used as received. Thin layer chromatography was performed on silica gel-coated plates (Kieselgel 60 F254, Merck, Germany) with the indicated solvent mixture, spots were detected by $KMnO_4$ staining (1.5 g $KMnO_4$, 10 g K_2CO_3, 2.5 mL 5% NaOH-solution, 150 mL H_2O), *p*-anisaldehyde staining (9.2 mL *p*-anisaldehyde, 321 mL EtOH, 17 mL H_2O, 3.75 mL AcOH, 12.7 mL H_2SO_4), and UV-detection. NMR spectra were recorded on a Bruker Biospin 400 (400 MHz) and a Bruker DMX300 (300 MHz). Protein mass spectra (HRMS) were recorded on a JEOL AccuTOF JMS-T100CS (Electrospray Ionization (ESI) time-of-flight) or a JEOL AccuTOF JMS-100GCv (Electron Ionization (EI), Chemical Ionization (CI)). Low-resolution mass spectra (LRMS) were recorded on a ThermoScientific Advantage LCQ Linear ion-trap electrospray or a Waters LCMS consisting of a 2767 Sample manager, 2525 pump, 2996 UV-detector, and a Micromass ZQ with an Xbridge C18 3.5 μm column (ESI).

DOI: 10.1021/acs.bioconjchem.5b00224
Bioconjugate Chem. 2015, 26, 2233–2242

3,4,6-Tri-*O*-acetyl-2-azido-2-deoxy-α-D-galactose-1-phosphate (9). Compound **9** was prepared from D-galactosamine according to the procedure described for D-glucosamine by Linhardt et al.[46] ^{1}H NMR (300 MHz, CD_3OD): δ 5.69 (dd, *J* = 7.2, 3.3 Hz, 1H), 5.43−5.42 (m, 1H), 5.35 (dd, *J* = 11.1, 3.3 Hz, 1H), 4.53 (t, *J* = 7.2 Hz, 1H), 4.21−4.13 (m, 1H), 4.07−4.00 (m, 1H), 3.82 (dt, *J* = 10.8, 2.7 Hz, 1H), 2.12 (s, 3H), 2.00 (s, 3H), 1.99 (s, 3H). LRMS (ESI-) calcd for $C_{12}H_{17}N_3O_{11}P$ (*M*-H$^-$) 410.06, found 410.00.

3,4,6-Tri-*O*-acetyl-α-D-galactosamine-1-phosphate (10). To a solution of azide **9** (105 mg, 0.26 mmol) in MeOH (3 mL) was added Pd/C (20 mg). The reaction was stirred under a hydrogen atmosphere for 2 h and filtered over Celite. The filter was rinsed with MeOH (10 mL) and the filtrate was concentrated in vacuo to afford free amine **10** (94 mg, 0.244 mmol, 96%). ^{1}H NMR (300 MHz, D_2O): δ 5.87−5.76 (m, 1H), 5.44 (br s, 1H), 5.30−5.20 (m, 1H), 4.55 (t, *J* = 6.3 Hz, 1H), 4.28−4.00 (m, 3H), 2.11 (s, 3H), 2.03 (s, 3H), 2.00 (s, 3H). LRMS (ESI$^-$) calcd for $C_{12}H_{19}NO_{11}P$ (*M*-H$^-$) 384.07, found 384.10.

3,4,6-Tri-*O*-acetyl-*N*-(2′-azido-2′,2′-difluoroacetyl)-α-D-galactosamine-1-phosphate (11). To a solution of amine **10** (94 mg, 0.244 mmol) in dry DMF (3 mL) were added ethyl difluoroazidoacetate (48 mg, 0.293 mmol) and Et_3N (68 μL, 0.49 mmol). The reaction was stirred for 6 h at r.t., followed by concentration in vacuo to afford the crude product. Flash chromatography (100:0−50:50 EtOAc:MeOH) afforded product **11** (63 mg, 0.125 mmol, 51%). ^{1}H NMR (300 MHz, CD_3OD): δ 5.64 (m, 1H), 5.47 (d, *J* = 2.4 Hz, 1H), 5.35 (dd, *J* = 11.4, 3.0 Hz, 1H), 4.58−4.48 (m, 2H), 4.25−4.15 (m, 1H), 4.09−4.00 (m, 1H), 2.14 (s, 3H), 2.00 (s, 3H), 1.93 (s, 3H). LRMS (ESI-) calcd for $C_{14}H_{18}F_2N_4O_{12}P$ (*M*-H$^-$) 503.06, found 503.0.

UDP 3,4,6-Tri-*O*-acetyl-2-(2′-azido-2′,2′-difluoroacetyl)-)-α-D-galactosamine (12). Monophosphate **11** was coupled to UMP according to the procedure reported by Baisch et al.[47] Thus, a solution of D-uridine-5′-monophosphate disodium salt (98 mg, 0.266 mmol) in H_2O (1 mL) was treated with DOWEX 50Wx8 (H^+ form) for 40 min and filtered. The filtrate was stirred vigorously at r.t. while tributylamine (63 μL, 0.266 mmol) was added dropwise. After 30 min of stirring, the reaction mixture was lyophilized and further dried over P_2O_5 under vacuum for 5 h.

The resulting tributylammonium uridine-5′-monophosphate was dissolved in dry DMF (15 mL) under an argon atmosphere. 1,1′- Carbonyldiimidazole (35 mg, 0.219 mmol) was added and the reaction mixture was stirred at r.t. for 30 min. Next, dry MeOH (4.63 μL) was added and the reaction was stirred for 15 min to remove the excess carbonyl diimidazole. The leftover MeOH was removed under high vacuum for 15 min. Subsequently, *N*-methylimidazole, HCl salt (61 mg, 0.52 mmol) was added to the reaction mixture and the monophosphate **11** (63 mg, 0.125 mmol) was dissolved in dry DMF (15 mL) and added dropwise to the reaction mixture. The reaction was allowed to stir at r.t. overnight before concentration in vacuo. The consumption of the imidazole-UMP intermediate was monitored by MS. Flash chromatography (7:2:1−5:2:1 EtOAc:MeOH:H_2O) afforded the product **12**. ^{1}H NMR (300 MHz, D_2O): δ 7.87 (d, *J* = 8.1 Hz, 1H), 5.913−5.85 (m, 2H), 5.67 (dd, *J* = 6.6, 2.7 Hz, 1H), 5.56−5.50 (m, 1H), 5.47−5.43 (m, 1H), 5.31−5.25 (m, 2H), 4.61−4.43 (m, 2H), 4.31−4.05 (m, 5H), 2.16 (s, 3H), 2.02 (s, 3H), 1.94 (s, 3H). LRMS (ESI$^-$) calcd for $C_{23}H_{29}F_2N_6O_{20}P_2$ (*M*-H$^-$) 809.09, found 809.1.

UDP 2-(2′-Azido-2′,2′-difluoroacetyl)-α-D-galactosamine (UDP-F_2−GalNAz, 4). Compound **12** was dissolved in H_2O (1 mL) and triethylamine (1 mL) and MeOH (2.4 mL) were added. The reaction mixture was stirred for 2 h and then concentrated in vacuo. Flash chromatography (7:2:1−5:2:1 EtOAc:MeOH:H_2O) afforded UDP F_2−GalNAz (**4**; Scheme 1). ^{1}H NMR (300 MHz, D_2O): δ 7.86 (d, *J* = 8.1 Hz, 1H),

Scheme 1. Synthesis of UDP-Sugars 4 and 5

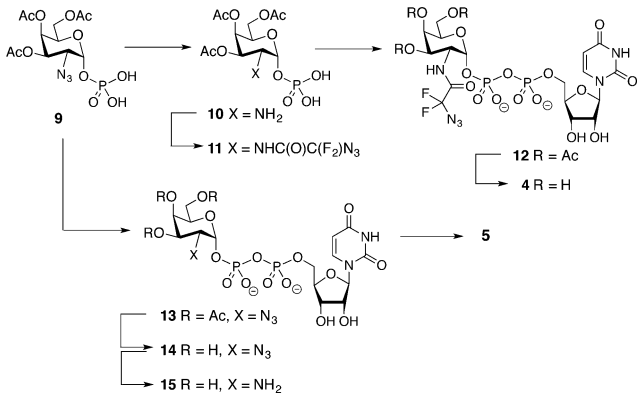

5.91−5.85 (m, 2H), 5.54 (dd, *J* = 6.6, 3.6 Hz, 1H), 4.31−3.95 (m, 9H), 3.74−3.62 (m, 2H). LRMS (ESI$^-$) calcd for $C_{17}H_{23}F_2N_6O_{17}P_2$ (*M*-H$^-$) 683.06, found 683.10.

UDP 3,4,6-Tri-*O*-acetyl-2-azido-2-deoxy-α-D-galactose (13). To a solution of D-uridine-5′-monophosphate disodium salt (1.49 g, 4.05 mmol) in H_2O (15 mL) was treated with DOWEX 50Wx8 (H^+ form) for 30 min and filtered. The filtrate was stirred vigorously at room temperature while tributylamine (0.966 mL, 4.05 mmol) was added dropwise. After 30 min of further stirring, the reaction mixture was lyophilized and further dried over P_2O_5 under vacuum for 5 h.

The resulting tributylammonium uridine-5′-monophosphate was dissolved in dry DMF (25 mL) under an argon atmosphere. Carbonyldiimidazole (1.38 g, 8.51 mmol) was added and the reaction mixture was stirred at r.t. for 30 min. Next, dry MeOH (180 μL) was added and the reaction was stirred for 15 min to remove the excess carbonyldiimidazole. The leftover MeOH was removed under high vacuum for 15 min. Subsequently, compound **9** (2.0 g, 4.86 mmol) was dissolved in dry DMF (25 mL) and added dropwise to the reaction mixture. The reaction was allowed to stir at r.t. for 2 d before concentration in vacuo. The consumption of the imidazole-UMP intermediate was monitored by MS. Flash chromatography (7:2:1−5:2:1 EtOAc:MeOH:H_2O) afforded product **13** (1.08 g, 1.51 mmol, 37%). ^{1}H NMR (300 MHz, D_2O): δ 7.96 (d, *J* = 8.0 Hz, 1H), 5.98−5.94 (m, 2H), 5.81−5.79 (m, 1H), 5.70 (dd, *J* = 7.1, 3.3 Hz, 1H), 5.49 (dd, *J* = 15.2, 2.6 Hz, 1H), 5.30 (ddd, *J* = 18.5, 11.0, 3.2 Hz, 2H), 4.57 (q, *J* = 6.0 Hz, 2H), 4.35−4.16 (m, 9H), 4.07−3.95 (m, 2H), 2.17 (s, 3H), 2.08 (s, 3H), 2.07 (s, 3H). LRMS (ESI$^-$) calcd for $C_{21}H_{29}N_5O_{19}P_2$ (*M*-H$^-$) 716.09, found 716.3.

UDP 2-Azido-2-deoxy-α-D-galactose (14). Compound **13** (222 mg, 0.309 mmol) was dissolved in H_2O (2.5 mL) and triethylamine (2.5 mL) and MeOH (6 mL) were added. The reaction mixture was stirred for 3 h at r.t. and then concentrated in vacuo to afford crude **14**. ^{1}H NMR (300 MHz, D_2O): δ 7.99 (d, *J* = 8.2 Hz, 1H), 6.02−5.98 (m, 2H),

DOI: 10.1021/acs.bioconjchem.5b00224
Bioconjugate Chem. 2015, 26, 2233−2242

5.73 (dd, J = 7.4, 3.4 Hz, 1H), 4.42−4.37 (m, 2H), 4.30−4.18 (m, 4H), 4.14−4.04 (m, 2H), 3.80−3.70 (m, 2H), 3.65−3.58 (m, 1H). LRMS (ESI$^-$) calcd for $C_{15}H_{23}N_5O_{16}P_2$ (M-H$^-$) 590.05, found 590.2.

UDP α-D-Galactosamine (15). To a solution of compound **14** in H_2O:MeOH 1:1 (4 mL) was added Lindlar's catalyst (50 mg). The reaction was stirred under a hydrogen atmosphere for 5 h and filtered over Celite. The filter was rinsed with H_2O (10 mL) and the filtrate was concentrated in vacuo to afford **15** (169 mg, 0.286 mmol, 92% yield over two steps). ^{1}H NMR (300 MHz, D_2O): δ 7.93 (d, J = 8.1 Hz, 1H), 5.99−5.90 (m, 2H), 5.76−5.69 (m, 1H), 4.39−4.34 (m, 2H), 4.31−4.17 (m, 5H), 4.05−4.01 (m, 1H), 3.94−3.86 (m, 1H), 3.82−3.70 (m, 3H), 3.30−3.16 (m, 1H). LRMS (ESI$^-$) calcd for $C_{15}H_{25}N_3O_{16}P_2$ (M-H$^-$) 564.06, found 564.1.

UDP 2-(4′-Azido-3′,5′-difluorobenzoyl)-α-D-galactosamine (UDP F_2−GalNBAz, 5). To a solution of 4-azido-3,5-difluorobenzoic acid was added dicyclohexylcarbodiimide (1.1 equiv) and N-hydroxysuccinimide (1.2 equiv) and the resulting suspension was stirred overnight at r.t. followed by vacuum filtration. The filtrate was concentrated and dissolved in EtOAc followed by washing with saturated $NaHCO_3$ (aq.) and brine. The organic layer was dried over Na_2SO_4, filtrated, and concentrated in vacuo to use crude in the next reaction. ^{1}H NMR (300 MHz, $CDCl_3$): δ 7.74−7.66 (m, 2H), 2.91 (s, 4H).

Next, UDP GalNH$_2$ (**15**, 30 mg, 0.0531 mmol) was dissolved in 0.1 M $NaHCO_3$ (0.2 M) and the N-hydroxysuccinimide ester of 4-azido-3,5-difluorobenzoic acid (31 mg, 0.106 mmol, 2 equiv), dissolved in DMF (0.2 M), was added. The reaction was stirred overnight at r.t. and concentrated in vacuo. Flash chromatography (7:2:1−5:2:1 EtOAc:MeOH:H_2O) afforded product **5** (8 mg, 0.011 mmol, 20%). ^{1}H NMR (300 MHz, D_2O): δ 7.73 (d, J = 8.4 Hz, 1H), 7.52−7.31 (m, 2H), 5.87−5.71 (m, 2H), 5.65−5.57 (m, 1H), 5.47−5.33 (m, 1H), 4.43−3.96 (m, 8H), 3.76−3.60 (m, 2H). LRMS (ESI$^-$) calcd for $C_{22}H_{25}F_2N_6O_{17}P_2$ (M-H$^-$) 745.07, found 744.9.

General Protocol for Mass Spectral Analysis of IgG. Prior to mass spectral analysis, IgGs were either treated with DTT, which allows analysis of both light and heavy chain, or treated with Fabricator (commercially available from Genovis, Lund, Sweden), which allows analysis of the Fc/2 fragment. For analysis of both light and heavy chain, a solution of 20 μg (modified) IgG was incubated for 5 min at 37 °C with 100 mM DTT in a total volume of 4 μL. If present, azide-functionalities are reduced to amines under these conditions. For analysis of the Fc/2 fragment, a solution of 20 μg (modified) IgG was incubated for 1 h at 37 °C with Fabricator (1.25 U/μL) in phosphate-buffered saline (PBS) pH 6.6 in a total volume of 10 μL. After reduction with DTT or Fabricator-digestion the samples were washed trice with Milli-Q using an Amicon Ultra-0.5, Ultracel-10 Membrane (Millipore) resulting in a final sample volume of approximately 40 μL. Next, the samples were analyzed by electrospray ionization time-of-flight (ESI-TOF) on a JEOL AccuTOF. Deconvoluted spectra were obtained using *Magtran* software.

Glycan Trimming of Trastuzumab with Endo S. Trastuzumab **I** (10−20 mg/mL) was incubated with endo S from *Streptococcus pyogenes* (4 U/mg IgG, commercially available as IgGZERO from Genovis, Lund, Sweden) in 25 mM Tris pH 8.0 for 16 h at 37 °C. Next, trimmed IgG (**II**) was concentrated and washed with 10 mM $MnCl_2$ and 25 mM Tris-HCl pH 8.0 using an Amicon Ultra-0.5, Ultracel-10 Membrane (Millipore).

After deconvolution of peaks, the mass spectrum showed one peak of the light chain and two peaks of the heavy chain. The two peaks of heavy chain belong to one major product (49 496 Da, 90% of total heavy chain), resulting from core GlcNAc-(Fuc) substituted trastuzumab, and a minor product (49 351 Da, ±10% of total heavy chain), resulting from trimmed trastuzumab lacking L-fucose.

Protocol for Glycosyltransfer of UDP-GalNAz (2) or UDP-F_2−GalNAz (4) with GalT(Y289L) to Obtain III-2 or III-4. Trimmed trastuzumab **II** (10 mg/mL) was incubated with the appropriate UDP-GalNAc derivative **2** (commercially available from CarboSynth, Compton, Berkshire, UK) or **4** (0.4 mM) and β(1,4)-Gal-T1(Y289L)[48] (0.1 mg/mL) in 10 mM $MnCl_2$ and 25 mM Tris-HCl pH 8.0 for 16 h at 30 °C. Next, the functionalized trastuzumab was purified on a HiTrap MabSelect SuRe 5 mL column (GE Healthcare) using an AKTA purifier-10 (GE Healthcare). The eluted IgG was immediately neutralized with 1.5 M Tris-HCl pH 8.8 and dialyzed against PBS pH 7.4. Next the IgG was concentrated using an Amicon Ultra-0.5, Ultracel-10 Membrane (Millipore) to a concentration of 20 mg/mL.

Mass spectral analysis of **III-2** after reduction with DTT indicated the formation of one major product (49 713 Da, 90% of total heavy chain), resulting from GalNAz transfer to core GlcNAc(Fuc) substituted trastuzumab, and a minor product (49 566 Da, ±10% of total heavy chain), resulting from GalNAz transfer to core GlcNAc substituted trastuzumab.

Mass spectral analysis of **III-4** after reduction with DTT indicated the formation of one major heavy chain product (49 865 Da, approximately 90% of total heavy chain), resulting from F_2−GalNAz transfer to core GlcNAc(Fuc)-substituted trastuzumab which has subsequently reacted with DTT during sample preparation.

Preparation of Trastuzumab-(F_2−GalNBAz), III-5. Trimmed trastuzumab **II** (10 mg/mL) was incubated with UDP F_2−GalNBAz **5** (5 mM) and β(1,4)-Gal-T1(Y289M) (1 mg/mL) in 10 mM $MnCl_2$ and 25 mM Tris-HCl pH 8.0 at 30 °C overnight. Mass spectral analysis of a DTT-reduced sample indicated the formation of a one major product (49 813 Da, approximately 90% of total heavy chain), resulting from F_2−GalNBAz transfer to core GlcNAc(Fuc) substituted trastuzumab heavy chain.

General Protocol for Conjugation of Cyclooctyne Constructs (BCN/DBCO) to azido-mAbs III. Three volumes of a solution of the appropriate trastuzumab(azide)$_2$ **III** (20 mg/mL in PBS pH 7.4) were added to one volume of a solution containing the BCN/DBCO compound (≥1.2 mM solution in Milli-Q and/or organic cosolvent). Analytical scale reactions were performed at 10 μL scale and samples were taken at preset time points. Mass spectral analysis was performed as described above to determine the conjugation efficiency (see Table 1).

Preparative scale reactions were purified on a Superdex 200 10/300 GL (GE Healthcare) using an AKTA purifier-10 (GE Healthcare).

■ ASSOCIATED CONTENT

Supporting Information

Experimental procedures for the syntheses of compounds **7a−c** and **8a−c**, conjugation of **6−8** to trastuzumab(GalNAz)$_2$ and analysis, preparation and analysis of ADCs, protocols for in vitro and in vivo studies, and competition experiments. The Supporting Information is available free of charge on the ACS

DOI: 10.1021/acs.bioconjchem.5b00224
Bioconjugate Chem. 2015, 26, 2233−2242

Publications website at DOI: 10.1021/acs.bioconjchem.5b00224.

AUTHOR INFORMATION

Corresponding Author

*E-mail: F.vanDelft@SynAffix.com.

Notes

The authors declare the following competing financial interest(s): all authors are or have been (except A.A.W.) employees of SynAffix B.V.

ACKNOWLEDGMENTS

The work presented here is partially supported by a Stichting Technische Wetenschappen (STW) Valorization Grant (12305). Louis Boon from Bioceros (Utrecht, The Netherlands) is acknowledged for providing trastuzumab-containing supernatant.

REFERENCES

(1) Mathé, G., Loc, T. B., and Bernard, J. (1958) Effet sur la leucémie 1210 de la souris d'une combinaison par diazotation d'A-méthoptérine et de γ-globulines de hamsters porteurs de cette leucémie par hétérogreffe. *Compt. Rendu Acad. Sci. (Paris) 246*, 1626−8.

(2) Himmelweit, F. (1960) *The Collected Papers of Paul Ehrlich*, p 59, Vol. 3, Pergamon, London.

(3) Chari, R. V. J., Miller, M. L., and Widdison, W. C. (2014) Antibody−Drug Conjugates: An Emerging Concept in Cancer Therapy. *Angew. Chem., Int. Ed. 53*, 3796−827.

(4) Junutula, J. R., Raab, H., Clark, S., Bhakta, S., Leipold, D. D., Weir, S., Chen, Y., Simpson, M., Tsai, S. P., Dennis, M. S., Lu, Y., Meng, Y. G., Ng, C., Yang, J., Lee, C. C., Duenas, E., Gorrell, J., Katta, V., Kim, A., McDorman, K., Flagella, K., Venook, R., Ross, S., Spencer, S. D., Wong, W. L., Lowman, H. B., Vandlen, R., Sliwkowski, M. X., Scheller, R. H., Polakis, P., and Mallet, M. (2008) Site-specific conjugation of a cytotoxic drug to an antibody improves the therapeutic index. *Nat. Biotechnol. 26*, 925−32.

(5) Krop, I. E., Beeram, M., Modi, S., Jones, S. F., Holden, S. N., Yu, W., Girish, S., Tibbitts, J., Yi, J.-H., Sliwkowski, M. X., Jacobson, F., Lutzker, S. G., and Burris, H. A. (2010) Phase I study of trastuzumab-DM1, an HER2 antibody-drug conjugate, given every 3 weeks to patients with HER2-positive metastatic breast cancer. *J. Clin. Oncol. 28*, 2698−704.

(6) Beeram, M., Krop, I. E., Burris, H. A., Girish, S. R., Yu, W., Lu, M. W., Holden, S. N., and Modi, S. (2012) A phase 1 study of weekly dosing of trastuzumab emtansine (T-DM1) in patients with advanced human epidermal growth factor 2−positive breast cancer. *Cancer 118*, 5733−40.

(7) Shen, B.-Q., Xu, K., Liu, L., Raab, H., Bhakta, S., Kenrick, M., Parsons-Reponte, K. L., Tien, J., Yu, S.-F., Mai, E., Li, D., Tibbitts, J., Baudys, J., Saad, O. M., Scales, S. J., McDonald, P. J., Hass, P. E., Eigenbrot, C., Nguyen, T., Solis, W. A., Fuji, R. N., Flagella, K. M., Patel, D., Spencer, S. D., Khawli, L. A., Ebens, A., Wong, W. L., Vandlen, R., Kaur, S., Sliwkowski, M. X., Scheller, R. H., Polakis, P., and Junutula, J. R. (2012) Conjugation site modulates the in vivo stability and therapeutic activity of antibody-drug conjugates. *Nat. Biotechnol. 30*, 184−9.

(8) Lyon, R. P., Setter, J. R., Bovee, T. D., Doronina, S. O., Hunter, J. H., Anderson, M. E., Balasubramanian, C. L., Duniho, S. M., Leiske, C. I., Li, F., and Senter, P. D. (2014) Self-hydrolyzing maleimides improve the stability and pharmacological properties of antibody-drug conjugates. *Nat. Biotechnol. 32*, 1059−1062.

(9) Tumey, L. N., Charati, M., He, T., Sousa, E., Ma, D., Han, X., Clark, T., Casavant, J., Loganzo, F., Barletta, F., Lucas, J., and Graziani, E. I. (2014) Mild method for succinimide hydrolysis on ADCs: impact on ADC potency, stability, exposure, and efficacy. *Bioconjugate Chem. 25*, 1871−80.

(10) Aggerwal, P., and Bertozzi, C. R. (2014) Site-specific antibody−drug conjugates: the nexus of bioorthogonal chemistry, protein engineering, and drug development. *Bioconjugate Chem. 53*, 176−92.

(11) For example, an extensive optimization process to avoid formation of triple light chain antibody format of a THIOmab did not afford titers above 2 g/L, whereas for regular IgG yields of 3−5 g/L are customary. Gomez, N., Ouyang, J., Nguyen, M. D. H., Vinson, A. R., Lin, A. A., and Yuk, I. H. (2010) Effect of temperature, pH, dissolved oxygen, and hydrolysate on the formation of triple light chain antibodies in cell culture. *Biotechnol. Prog. 26*, 1438−45.

(12) Tian, F., Lu, Y., Manibusan, A., Sellers, A., Tran, H., Sun, Y., Phuong, T., Barnett, R., Hehli, B., Song, F., DeGuzman, M. J., Ensari, S., Pinkstaff, J. K., Sullivan, L. M., Biroc, S. L., Cho, H., Schultz, P. G., DiJoseph, J., Dougher, M., Ma, D., Dushin, R., Leal, M., Tchistiakova, L., Feyfant, E., Gerber, H. P., and Sapra, P. (2014) A general approach to site-specific antibody drug conjugates. *Proc. Natl. Acad. Sci. U. S. A. 111*, 1766−71.

(13) Zimmerman, E. S., Heibeck, T. H., Gill, A., Li, X., Murray, C. J., Madlansacay, M. R., Tran, C., Uter, N. T., Yin, G., Rivers, P. J., Yam, A. Y., Wang, W. D., Steiner, A. R., Bajad, S. U., Penta, K., Yang, W., Hallam, T. J., Thanos, C. D., and Sato, A. K. (2014) Production of site-specific antibody−drug conjugates using optimized non-natural amino acids in a cell-free expression system. *Bioconjugate Chem. 25*, 351−61.

(14) Fontaine, S. D., Reid, R., Robinson, L., Ashley, G. W., and Santi, D. V. (2014) Long-term stabilization of maleimide−thiol conjugates. *Bioconjugate Chem. 26*, 145−52.

(15) Beck, A., Wagner-Rousset, E., Ayoub, D., Van Dorsselaer, A., and Sanglier-Cianférani, S. (2013) Characterization of therapeutic antibodies and related products. *Anal. Chem. 85*, 715−36.

(16) Goetze, A. M., Liu, Y. D., Zhang, Z., Shah, B., Lee, E., Bondarenko, P. V., and Flynn, G. C. (2011) High-mannose glycans on the Fc region of therapeutic IgG antibodies increase serum clearance in humans. *Glycobiology 21*, 949−59.

(17) Ferrara, C., Grau, S., Jäger, C., Sondermann, P., Brünker, P., Waldhauer, I., Hennig, M., Ruf, A., Rufer, A. C., Stihle, M., Umaña, P., and Benz, J. (2011) Unique carbohydrate-carbohydrate interactions are required for high affinity binding between FcgammaRIII and antibodies lacking core fucose. *Proc. Natl. Acad. Sci. U. S. A. 108*, 12669−74.

(18) For example, see discussion in Sazinsky, S. L., Ott, R. G., Silver, N. W., Tidor, B., Ravetch, J. V., Wittrup, K. D. (2008) Aglycosylated immunoglobulin G1 variants productively engage activating Fc receptors. *Proc. Natl. Acad. Sci. U.S.A. 105*, 20167−72.

(19) Gorovits, B., and Krinos-Fiorotti, C. (2013) Proposed mechanism of off-target toxicity for antibody-drug conjugates driven by mannose receptor uptake. *Cancer Immunol. Immunother. 62*, 217−23.

(20) Up to 5−7% of nonglycosylated mAb may also be present, depending on protein sequence and expression system.

(21) Qu, Z., Sharkey, R. M., Hansen, H. J., Shih, L. B., Govindan, S. V., Shen, J., Goldenberg, D. M., and Leung, S. (1998) Carbohydrates engineered at antibody constant domains can be used for site-specific conjugation of drugs and chelates. *J. Immunol. Meth. 213*, 131−44.

(22) Boeggeman, E., Ramakrishnan, B., Pasek, M., Manzoni, M., Puri, A., Loomis, K. H., Waybright, T. J., and Qasba, P. K. (2009) Site specific conjugation of fluoroprobes to the remodeled Fc N-glycans of monoclonal antibodies using mutant glycosyltransferases: application for cell-surface antigen detection. *Bioconjugate Chem. 20*, 1228−36.

(23) Zhu, Z., Ramakrishnan, B., Li, J., Wang, Y., Feng, Y., Prabakaran, P., Colantonio, S., Dyba, M. A., Qasba, P. K., and Dimitrov, D. S. (2014) Site-specific antibody-drug conjugation through an engineered glycotransferase and a chemically reactive sugar. *mAbs 6*, 1−11.

(24) Zeglis, B. M., Davis, C. B., Aggeler, R., Kang, H.-C., Chen, A., Agnew, B., and Lewis, J. S. (2013) An enzyme-mediated methodology for the site-specific radiolabeling of antibodies based on catalyst-free click chemistry. *Bioconjugate Chem. 24*, 1057−67.

(25) Li, X., Fang, T., and Boons, G.-J. (2014) Preparation of well-defined antibody−drug conjugates through glycan remodeling and

DOI: 10.1021/acs.bioconjchem.5b00224
Bioconjugate Chem. 2015, 26, 2233−2242

strain-promoted azide−alkyne cycloadditions. *Angew. Chem., Int. Ed. 53*, 7179−82.
(26) Exact numbering of amino acids differs per mAb.
(27) For an overview of different endo F glycosidase, see for example: http://www.sigmaaldrich.com/technical-documents/articles/biology/glycobiology/endoglycosidases.html (accessed on April 20th, 2015). Also, see the following review: Karamanos, Y. (2013) Endo-N-acetyl-β-D-glucosaminidases and peptide-N4-(N-acetyl-β-D-glucosaminyl) asparagineamidases: More than just tools. *Adv. Biochem. 1*, 81−99.
(28) Colin, M., and Olsen, A. (2001) EndoS, a novel secreted protein from *Streptococcus pyogenes* with endoglycosidase activity on human IgG. *EMBO J. 20*, 3046−55.
(29) Goodfellow, J. J., Baruah, K., Yamamoto, K., Bonomelli, C., Krishna, B., Harvey, D. J., Crispin, M., Scanlan, C. N., and Davis, B. G. (2012) An endoglycosidase with alternative glycan specificity allows broadened glycoprotein remodelling. *J. Am. Chem. Soc. 134*, 8030−3.
(30) Sjögren, J., Struwe, W. B., Cosgrave, E. F. J., Rudd, P. M., Stervander, M., Allhorn, M., Hollands, A., Nizet, V., and Collin, M. (2013) EndoS2 is a unique and conserved enzyme of serotype M49 group A *Streptococcus* that hydrolyses N-linked glycans on IgG and α1-acid glycoprotein. *Biochem. J. 455*, 107−18.
(31) Ramakrishnan, B., and Qasba, P. K. (2002) Structure-based design of β1,4-galactosyltransferase I (β4Gal-T1) with equally efficient N-acetylgalactosaminyltransferase activity. *J. Biol. Chem. 277*, 20833−9.
(32) Khidekel, N., Arndt, S., Lamarre-Vincent, N., Lippert, A., Poulin-Kerstien, K. G., Ramakrishnan, B., Qasba, P. K., and Hsieh-Wilson, L. C. (2003) A chemoenzymatic approach toward the rapid and sensitive detection of O-GlcNAc posttranslational modifications. *J. Am. Chem. Soc. 125*, 16162−3.
(33) Hang, H. C., Yu, C., Pratt, M. R., and Bertozzi, C. R. (2004) Probing glycosyltransferase activities with the Staudinger ligation. *J. Am. Chem. Soc. 126*, 6−7.
(34) Agard, N. J., Prescher, J. A., and Bertozzi, C. R. (2004) A strain-promoted [3 + 2] azide-alkyne cycloaddition for covalent modification of biomolecules in living systems. *J. Am. Chem. Soc. 126*, 15046−7.
(35) Debets, M. F., van Berkel, S. S., Dommerholt, J., Dirks, A. J., Rutjes, F. P. J. T., and van Delft, F. L. (2011) Bioconjugation with strained alkenes and alkynes. *Acc. Chem. Res. 44*, 805−15.
(36) Dommerholt, J., Schmidt, S., Temming, R., Hendriks, L. J., Rutjes, F. P. J. T., van Hest, J. C. M., Lefeber, D. J., Friedl, P., and van Delft, F. L. (2010) Readily accessible bicyclononynes for bioorthogonal labeling and three-dimensional imaging of living cells. *Angew. Chem., Int. Ed. 49*, 9422−5.
(37) Debets, M. F., van Berkel, S. S., Schoffelen, S., Rutjes, F. P. J. T., van Hest, J. C. M., and van Delft, F. L. (2010) Aza-dibenzocyclooctynes for fast and efficient enzyme PEGylation via copper-free (3 + 2) cycloaddition. *Chem. Commun. 46*, 97−9.
(38) We have no explanation for this unexpected observation at this point, but we speculate that back-folding of dibenzocyclooctyne onto the polyaromatic pyrene may potentially take place, thereby precluding the desired copper-free click reaction.
(39) Detailed synthesis and characterization can be found in the Supporting Information.
(40) Only degradation of maytansine, predominantly ester hydrolysis, was observed.
(41) Jung, S. T., Reddy, S. T., Kang, T. H., Borrok, M. J., Sandlie, I., Tucker, P. W., and Georgiou, G. (2010) A glycosylated IgG variants expressed in bacteria that selectively bind FcγRI potentiate tumour cell killing by monocyte-dendritic cells. *Proc. Natl. Acad. Sci. U.S.A. 201*, 604−9.
(42) Dommerholt, J., van Rooijen, O., Borrmann, A., Fonseca Guerra, C., Bickelhaupt, F. M., and van Delft, F. L. (2014) Highly accelerated inverse electron-demand cycloaddition of electron-deficient azides with aliphatic cyclooctynes. *Nat. Commun. 5*, DOI: 10.1038/ncomms6378.
(43) Strop, P., Liu, S. H., Dorywalska, M., Delaria, K., Dushin, R. G., Tran, T. T., Ho, W. H., Farias, S., Casas, M. G., Abdiche, Y., Zhou, D., Chandrasekaran, R., Samain, C., Loo, C., Rossi, A., Rickert, M., Krimm, S., Wong, T., Chin, S. M., Yu, J., Dilley, J., Chaparro-Riggers, J., Filzen, G. F., O'Donnell, C. J., Wang, F., Myers, J. S., Pons, J., Shelton, D. L., and Rajpal, A. (2013) Location matters: site of conjugation modulates stability and pharmacokinetics of antibody drug conjugates. *Chem. Biol. 20*, 161−7.
(44) Dorywalska, M., Strop, P., Melton-Witt, J. A., Hasa-Moreno, A., Farias, S. E., Galindo Casas, M., Delaria, K., Lui, V., Poulsen, K., Loo, C., Krimm, S., Bolton, G., Moine, L., Dushin, R., Tran, T.-T., Liu, S.-H., Rickert, M., Foletti, D., Shelton, D. L., Pons, J., and Rajpal, A. (2015) Effect of attachment site on stability of cleavable antibody drug conjugates. *Bioconjugate Chem.*, DOI: 10.1021/bc5005747.
(45) Neither endo S nor endo S2 could be used in this case since both are only hydrolytically active on the native glycosylation site of IgGs.
(46) Masuko, S., Bero, S., Green, D. E., Weïwer, M., Liu, J., DeAngelis, P. L., and Linhardt, R. J. (2012) Chemoenzymatic synthesis of uridine diphosphate-GlcNAc and uridine diphosphate-GalNAc analogs for the preparation of unnatural glycosaminoglycans. *J. Org. Chem. 77*, 1449−56.
(47) Baisch, G., and Öhrlein, R. (1997) Convenient chemoenzymatic synthesis of β-purine-diphosphate sugars (GDP-fucose-analogues). *Bioorg. Med. Chem. 5*, 383−91.
(48) Boeggeman, E. E., Ramakrishnan, B., and Qasba, P. K. (2003) The N-terminal stem region of bovine and human β-1,4-galactosyltransferase I increases the in vitro folding efficiency of their catalytic domain from inclusion bodies. *Protein Expression Purif. 30*, 219−29.

DOI: 10.1021/acs.bioconjchem.5b00224
Bioconjugate Chem. 2015, 26, 2233−2242